

LYSOSOMES IN THE RAT SCIATIC NERVE FOLLOWING CRUSH

ERIC HOLTZMAN and ALEX B. NOVIKOFF

From the Department of Pathology, Albert Einstein College of Medicine, New York

ABSTRACT

Peripheral nerves undergoing degeneration are favorable material for studying the types, origins, and functions of lysosomes. The following lysosomes are described: (a) *Autophagic vacuoles* in altered Schwann cells. Within these vacuoles the myelin and much of the axoplasm which it encloses in the normal nerve are degraded (Wallerian degeneration). The delimiting membranes of the vacuoles apparently form from myelin lamellae. Considered as possible sources of their acid phosphatase are Golgi vesicles (primary lysosomes), lysosomes of the dense body type, and the endoplasmic reticulum which lies close to the vacuoles. (b) *Membranous bodies* that accumulate focally in myelinated fibers in a zone extending 2 to 3 mm distal to the crush. These appear to arise from the endoplasmic reticulum in which demonstrable acid phosphatase activity increases markedly within 2 hours after the nerve is crushed. (c) *Autophagic vacuoles* in the axoplasm of fibers proximal to the crush. The breakdown of organelles within these vacuoles may have significance for the reorganization of the axoplasm preparatory to regeneration. (d) *Phagocytic vacuoles* of altered Schwann cells. As myelin degeneration begins, some axoplasm is exposed. This is apparently engulfed by the filopodia of the Schwann cells, and degraded within the phagocytic vacuoles thus formed. (e) *Multivesicular bodies* in the axoplasm of myelinated fibers. These are generally seen near the nodes of Ranvier.

INTRODUCTION

Changes in nerve fibers following interruption of their connections with the perikarya have long been of interest to pathologists and cytologists, particularly since the work of Cajal (1). Recent electron microscope findings (2-5) suggested to us that the behavior of cell organelles might better be understood when the lysosomes in axoplasm and Schwann cells were investigated.

The biochemical concept of the lysosome (6) has now broadened into a general biological concept encompassing various aspects of intracellular digestive processes (reference 68; for a discussion of lysosomes in nerve cells, see reference 69). It is now recognized that lysosomes show a variety of morphological forms: digestive vacuoles resulting from phagocytosis or pinocytosis; autophagic

vacuoles in which sequestered areas of cytoplasm are degraded; bodies arising directly from the endoplasmic reticulum; residual bodies containing undigested residues; and primary lysosomes not yet in contact with materials to be digested (68, 7, 44, 69). All of these forms have been encountered in one or another of the cells we have studied after nerve crush: the Schwann cells distal to the crush, inside of which Wallerian degeneration of myelin occurs; the axoplasm of nerve fibers distal to the crush; the axoplasm proximal to the crush; and the histiocytes in the foreign body reaction tissue.

We have studied the lysosomes in frozen sections of appropriately fixed tissues incubated for acid phosphatase activity. The underlying assump-

tions in the use of this "marker" enzyme have been discussed elsewhere (6, 7).

MATERIALS AND METHODS

SURGICAL PROCEDURE: Female albino rats, weighing 200 to 300 gm, were anesthetized with ether, and a short region of one sciatic nerve was dissected free and crushed three times with a hemostat whose jaws were about 1 mm wide. A tight ligature, with a No. 3-0 thread, was placed around the crushed region, and the muscle and skin were sutured. With interruption of the nerve's continuity, degeneration ensues in the entire region distal to the crush.¹ The crush-ligature procedure keeps the nerve from curling and permits ready access to the site of injury.

FIXATION AND INCUBATION: The rats were sacrificed at intervals ranging from 1½ hours to 24 days after crush. Three to five nerves were studied by

¹ A short region of the nerve proximal to the crush undergoes similar changes.

electron microscopy, and considerably more by light microscopy, for each of these intervals: 1½ to 4 hours, 16 to 23 hours, 2 to 3 days, 5 to 7 days, and 12 to 24 days. Under Nembutal anesthesia, a ventral mid-line incision was made. The sciatic nerves were fixed by perfusion, through the abdominal aorta, of 2 to 4 per cent glutaraldehyde in 0.1 M cacodylate buffer (8) to which calcium was often added (9). This was done at 5°C, in the cold room. The fixative was at approximately 5°C, except for the first few ml which were warmed to 25°C. A perfusion head of 90 to 100 cm and a flow rate of 1 to 3 ml/min. (after an initial 2 to 3 minutes at 2 to 5 ml/min.) were maintained for about 20 minutes. Frequently, after the perfusion had been under way for several minutes, the nerve was exposed and flooded with fixative. After perfusion the nerve was excised and placed in fresh fixative, generally for 10 to 20 minutes. Segments of the nerve, both distal and proximal to the crush, were processed. Nerves from unoperated animals and the contralateral (unoperated) nerves from operated animals served as controls.

After glutaraldehyde fixation, the nerves were

Except where noted, all electron micrographs are of preparations fixed with glutaraldehyde, postfixed in osmium tetroxide, and stained with uranyl and lead. Except for Figs. 45, and 46, all material is from the distal segment of the nerve. Where incubated for acid phosphatase, the times of incubation are indicated in parentheses.

FIGURE 1 Portion of an unoperated nerve, including a node of Ranvier. In the axoplasm, reaction product is seen in the endoplasmic reticulum (*E*), membranous bodies (*MB*), and multivesicular body (*MV*). In the Schwann cell, it is seen in a dense body (*D*). Myelin is seen at *M*. (50 min.) × 12,500.

FIGURE 2 Portion of an unoperated nerve, near a node of Ranvier. Small dense bodies (*D*) are seen in the Schwann cell. Myelin is seen at *M*. × 24,000.

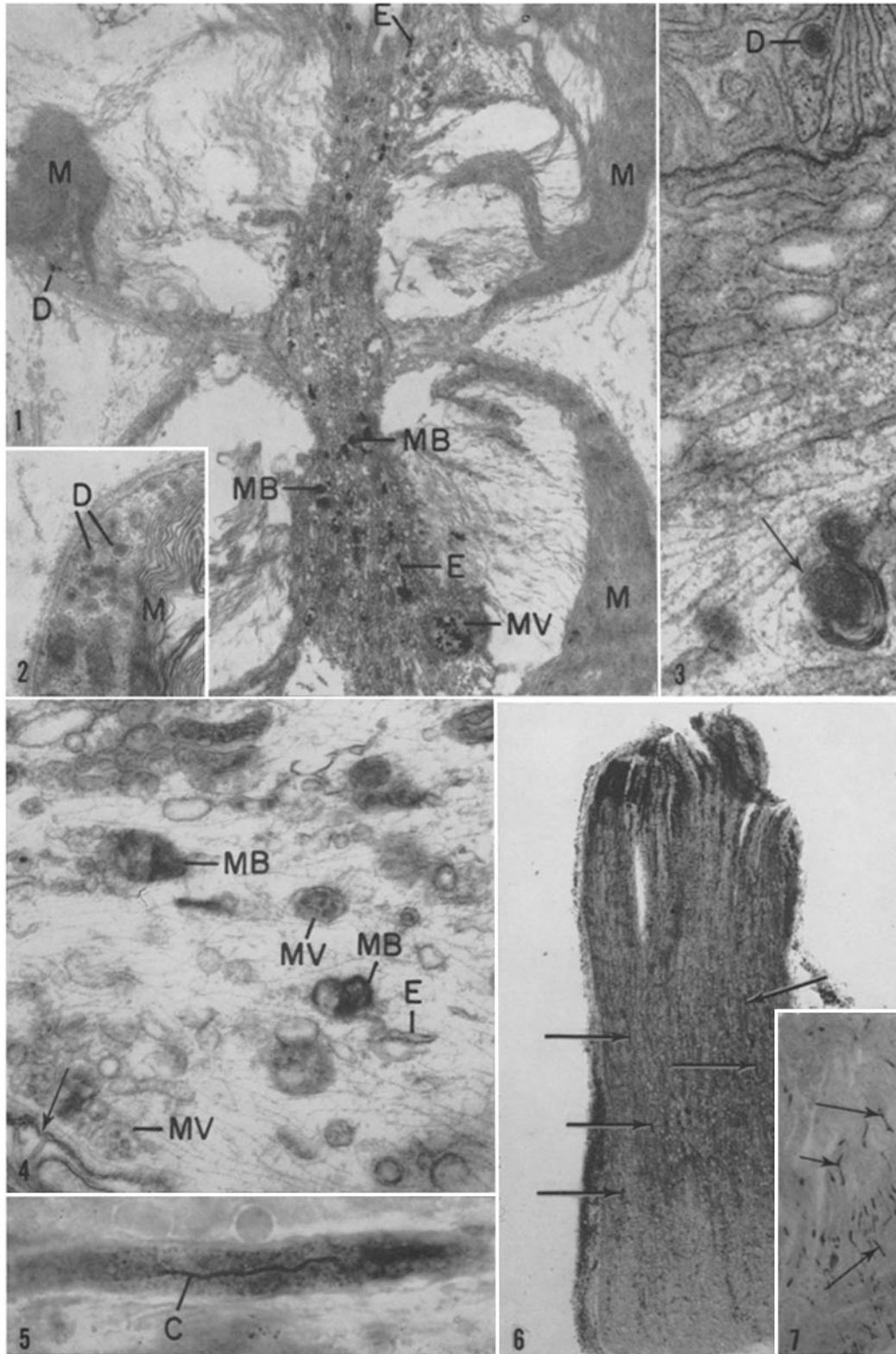
FIGURE 3 Portion of an unoperated nerve, at a node of Ranvier. A small dense body (*D*) is seen in the Schwann cell associated with the myelin loop. A membranous body is seen at the arrow. × 53,000.

FIGURE 4 Portion of an unoperated nerve, at a node of Ranvier. The typical configuration of myelin at the nodes is seen at the arrow. Within the axoplasm, note the endoplasmic reticulum (*E*), membranous bodies (*MB*), and multivesicular bodies (*MV*). × 36,000.

FIGURE 5 Portion of a fiber from the 2- to 3-mm zone in the distal nerve, 1 day after crush. Reaction product is present as small granules, core (*C*), and diffuse form. (35 min.) × 1350.

FIGURE 6 Portion of a nerve, 3 days after crush. The beginning of the crush area is barely evident, at the rounded end (above). Immediately distal to it is a zone of intensely stained fibers (see text). Distal to this is a zone where numerous myelinated fibers show reaction product in their axoplasm (arrows) (*cf.* Fig. 7). In the most distal zone, reaction product is not seen in the axoplasm or Schwann cells (see text). (30 min.) × 27.

FIGURE 7 Portion of the same nerve as used for Fig. 5. Reaction product (arrows) is seen in the axoplasm of many myelinated fibers. (35 min.) × 40.



rinsed in 0.1 M cacodylate buffer, pH 7.4, containing 7 per cent sucrose. In general, rinsing for $\frac{1}{2}$ to several hours appeared to give better myelin preservation than overnight rinses (*cf.* reference 9), but no differences in enzyme localizations were apparent. Sections were then cut with a freezing microtome set at 40 μ , and were collected in 7.5 per cent sucrose. They were incubated in a Gomori acid phosphatase medium (10) which had been kept at 37°C for 1 hour and filtered just before use. The medium contained 5 per cent sucrose and incubation was carried out at 37°C. Sample 40- μ sections were removed periodically and visualized in ammonium sulfide to monitor the course of the reaction. When they showed adequate accumulation of reaction product (usually after 20 to 50 minutes of incubation) the remaining sections were removed from the incubation medium and washed in 7.5 per cent sucrose. The visualized sections were used to locate the regions of the nerve where considerable reaction product had accumulated. These

regions were then removed from the unvisualized 40- μ sections, under a binocular microscope, and processed for electron microscopy. The 2 to 3 mm of the nerve distal to the crush showed the most extensive accumulations of reaction product (Figs. 6 and 7) (*cf.* reference 11).

Sections were incubated as enzyme controls in a complete medium with 0.01 M NaF and in a substrate-free medium (10).

ELECTRON MICROSCOPY: The trimmed 40- μ sections were postfixated for 30 minutes in 1 per cent OsO₄ in Veronal-acetate buffer, pH 7.4 (12), containing 4.5 per cent sucrose. Unincubated nerves were also prepared for electron microscopy; they were perfused, as described above, and postfixated for 1 to 3 hours. The tissues were dehydrated in ethanol and embedded in Araldite by the procedure of Luft (13). On several occasions sodium permanganate (14) was used in place of OsO₄ for postfixation.

Gray-to-light gold sections were cut on a Porter-

FIGURE 8 Portion of axoplasm of a myelinated fiber, 2 hours after crushing. Reaction product is seen in the smooth endoplasmic reticulum (arrows) and membranous bodies (*MB*); it is not present in the mitochondria (*MI*). Lead stained. (30 min.) \times 37,000.

FIGURE 9 Portion of a myelinated fiber, 2 hours after crushing. Note the absence of ribosomes on the surface of the smooth endoplasmic reticulum (arrow) and a moderately dense content in its interior. \times 37,500.

FIGURES 10 to 13 Portions of the axoplasm of myelinated fibers, 2 to 24 hours after crushing, with membranous bodies (arrows) attached to the endoplasmic reticulum (*E*). Note the microtubule (*T*) in Fig. 11 (*cf.* reference 65). Figs. 10 and 11, unincubated; Figs. 12 and 13, incubated, 30 and 35 min. respectively. Figs. 10 and 11, \times 57,500; Fig. 12, \times 60,500; Fig. 13, 46,000.

FIGURE 14 Degenerating mitochondria (*MI*) in the axoplasm of a myelinated fiber, 3 days after crushing. Note the dense granules (arrows). \times 45,000.

FIGURE 15 Portion of axoplasm in a myelinated fiber, 1 day after crushing. Numerous membranous bodies (arrows) and degenerating mitochondria (*MI*) are evident. \times 37,000.

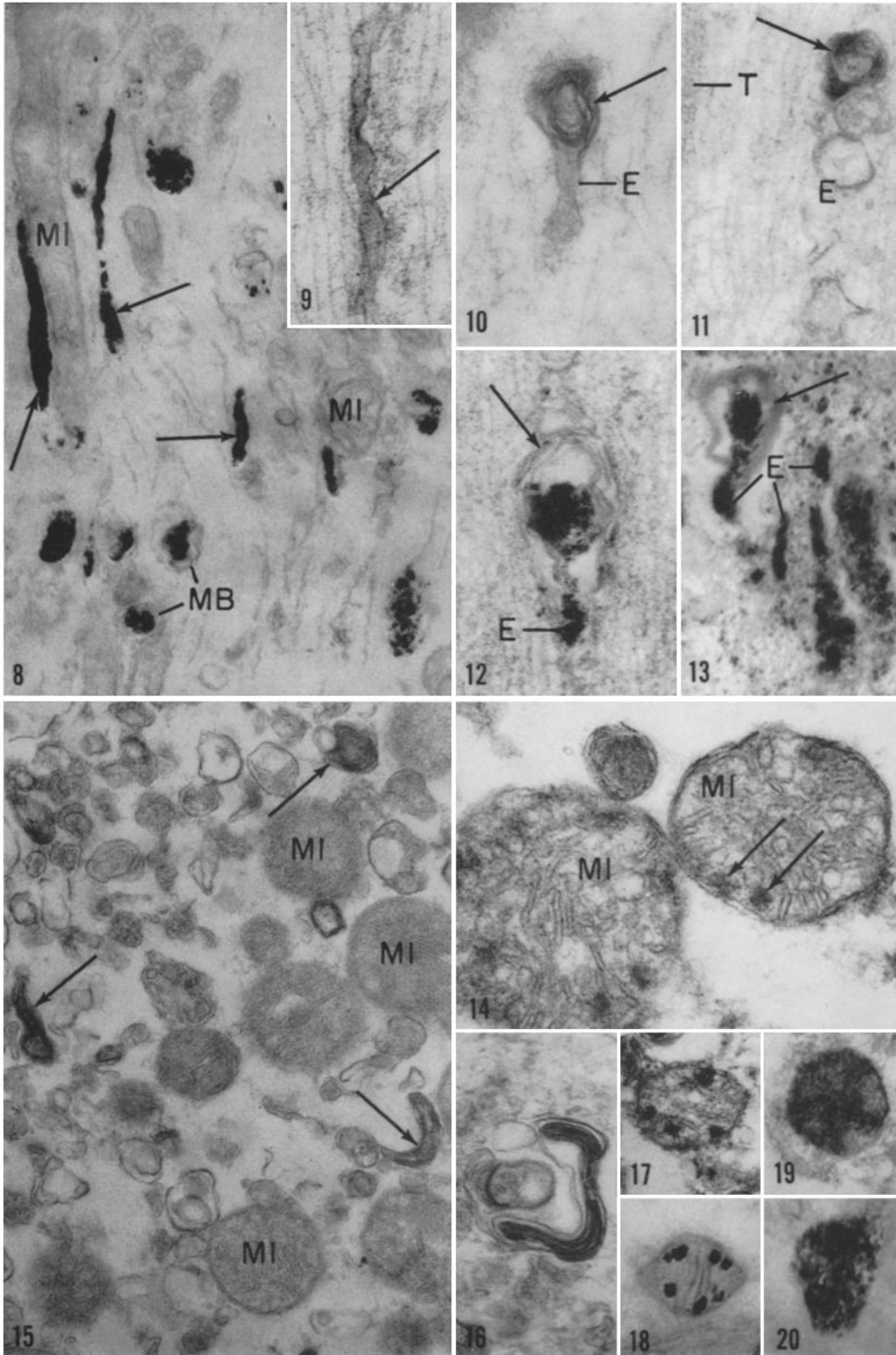
FIGURE 16 Membranous body from axoplasm of a myelinated fiber, 1 day after crushing, showing lamellar arrangement of membranes. \times 51,000.

FIGURE 17 Mitochondrion in a myelinated fiber, 1 day after crushing. Lead deposits are seen on the intramitochondrial granules. (30 min.) \times 52,000.

FIGURE 18 Mitochondrion in an unmyelinated fiber from the same nerve as Fig. 17. Intramitochondrial granules show dense lead deposits. Incubated in substrate-free medium (50 min.). \times 43,000.

FIGURE 19 Mitochondrion in a myelinated fiber, 3 days after crushing. A diffuse lead deposit is present. (30 min.) \times 26,000.

FIGURE 20 Mitochondrion in a myelinated fiber, 1 day after crushing. A diffuse lead deposit is present (*cf.* Fig. 19). The thin section was not stained. Incubated in substrate-free medium (50 min.). \times 53,000.



Blum microtome with glass or diamond knives. Sections were collected on uncoated copper grids and stained with alcoholic uranyl acetate (15), Reynolds's lead citrate (16), or with uranyl followed by lead. Comparison with unstained preparations showed that neither the lead nor the uranyl stains would be confused with enzyme reaction product, lead phosphate.

Sections were examined in a RCA EM 3B microscope operated at 100 kv. Photographs were taken at initial magnification of 2000 to 16,000.

RESULTS

Myelinated Fibers

The precise time course of degeneration in myelinated fibers distal to the crush varies along the length of the fiber, from fiber to fiber and, to some degree, from animal to animal (*cf.* references 3, 17). Most lysosomal changes occur within the first few days after crushing. Axoplasmic changes are first observed in some fibers an hour or two after crushing. By the second to third day most fibers show similar alterations. The formation of large myelin segments, the "ovoids" (1), occurs in a few fibers during the first day and in essentially all fibers by 3 days. The ovoids, surrounded by cytoplasm of transforming Schwann cells, fragment into smaller masses. These are enclosed within vacuoles which we refer to as "digestion vacuoles."² They are numerous after the third day. The myelin is changed into Marchi-positive (*cf.* reference 18) or Oil Red O-positive globules

² It is to be noted that these "digestion vacuoles" are not identical with Cajal's "digestion chambers" (1) which he considered to be the interior of the ovoids.

inside the digestion vacuoles. These globules are prominent from the sixth to twelfth days; beyond this period they become gradually less abundant.

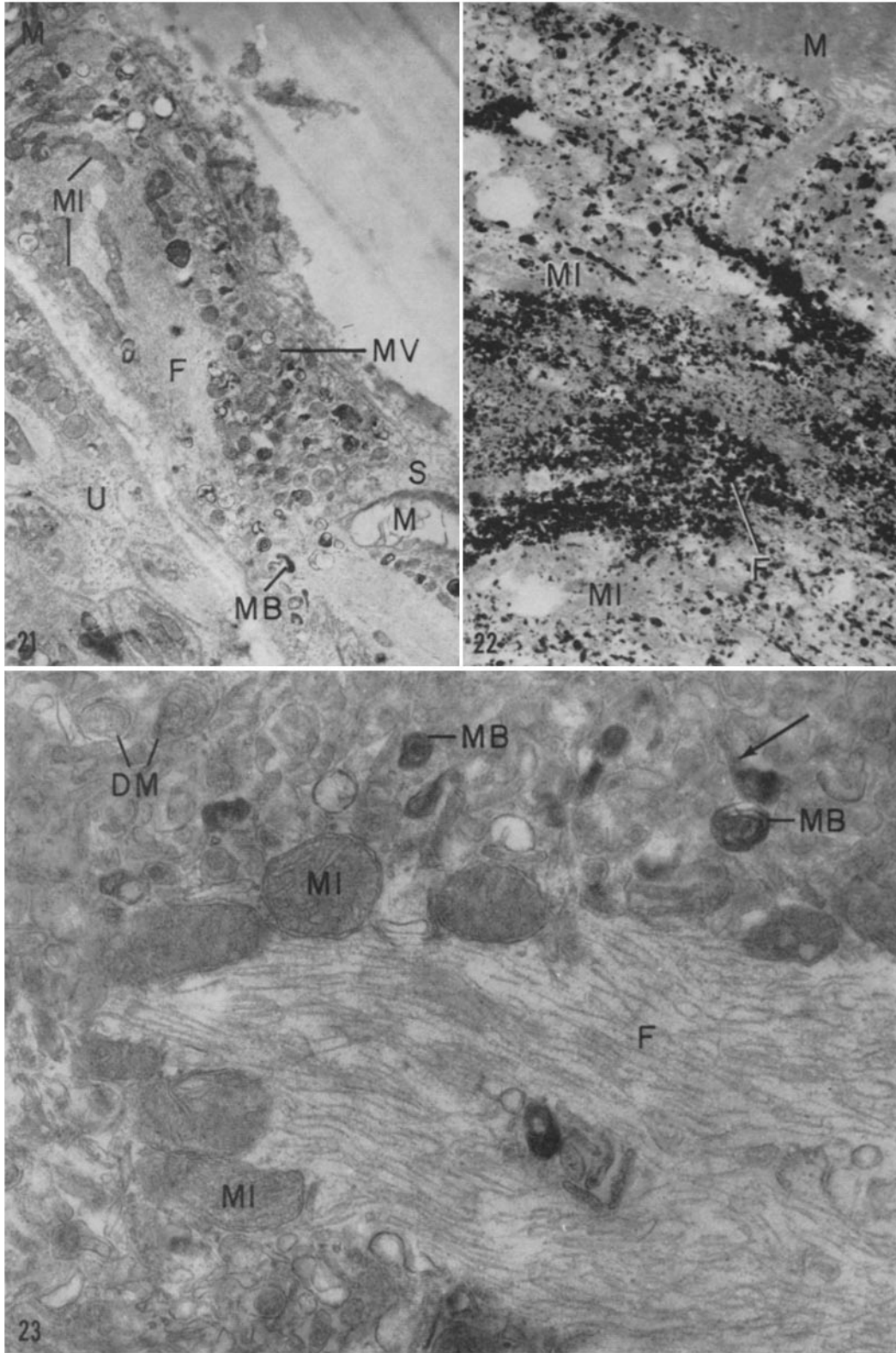
Light microscopy shows no acid phosphatase reaction product in the axoplasm of control (unoperated) nerves (*cf.* references 11, 19), except occasionally in small sites at the nodes of Ranvier. Electron microscopy shows these sites to include regions of tubular structures which we call smooth endoplasmic reticulum, "membranous bodies" (see below), and multivesicular bodies (20) (Figs. 1, 3, and 4). Rarely does electron microscopy reveal reaction product in the axoplasm away from the nodes; when it does, the product is in the endoplasmic reticulum and membranous bodies. In the Schwann cells, reaction product is found in the Golgi apparatus, in typical dense bodies, and, sometimes, in smaller dense bodies (20) concentrated near the node (Figs. 2 and 3).

Within 2 hours after injury, light microscopy shows focal accumulations of abundant acid phosphatase product in the axoplasm of myelinated fibers distal to the crush. By 3 days the nerve shows four distinct zones (Fig. 6). The first zone, the crush itself, has no acid phosphatase activity or other enzyme activities that we have studied (21). Immediately distal is a zone approximately 0.5 mm in length where intense acid phosphatase activity is evident. The next zone, 2 to 3 mm in length, shows many fibers with acid phosphatase in the axoplasm. This is the zone we have investigated most intensively. In the myelinated fibers of this region reaction product is sometimes concentrated in the paranodal axoplasm but frequently extends throughout the length of an inter-

FIGURE 21 Portion of a myelinated fiber at the node of Ranvier, 1 day after crushing. The myelin (*M*) has retracted from the node, leaving a denuded region of axoplasm in which aggregated neurofilaments (*F*), mitochondria (*MI*), membranous bodies (*MB*) and multivesicular bodies (*MV*) are present. One of the Schwann cells which originally covered the axoplasm at the node is seen at *S*. An unmyelinated fiber (*U*) is present at lower left. $\times 9500$.

FIGURE 22 Portion of axoplasm of a myelinated fiber, 1 day after crushing. Diffuse reaction product is concentrated in the aggregated neurofilaments (*F*). Neither mitochondria (*MI*) nor myelin (*M*) shows reaction product. (30 min.) $\times 17,500$.

FIGURE 23 Portion of axoplasm of a myelinated fiber, 1 day after crush. The neurofilaments (*F*) have aggregated in the center of the axoplasm. The other organelles are segregated to the periphery; note reasonably intact mitochondria (*MI*), degenerating mitochondria (*DM*), and membranous bodies (*MB*), one of which shows continuity with the endoplasmic reticulum at arrow. $\times 35,000$.



node or over even longer distances (Fig. 7). The remainder of the nerve shows no acid phosphatase activity in the axoplasm. We have not observed axoplasmic reaction product farther distal than approximately 3 mm at any stage of degeneration (*cf.* reference 11).

In the zone measuring 2 to 3 mm in length, light microscopy shows the axoplasmic reaction product in three forms: diffuse; granular; and in "cores" (Fig. 5). The electron microscope reveals that the diffuse form is due to enzyme product in smooth endoplasmic reticulum (Figs. 8 and 9). This is seen in many fibers within 2 hours after the crush; in striking contrast to the control nerves, it involves areas at considerable distances from the nodes.

The granular reaction product is associated with bodies that accumulate focally in the axo-

plasm (*cf.* reference 2). Because of their membranous or lamellar character (Figs. 10, 11, 15, and 16) we refer to them as "membranous bodies." This term is used to distinguish them from typical "dense bodies" encountered in the Schwann cell (Figs. 36 and 41) and from bodies that arise from degenerating mitochondria (Fig. 23). The membranous bodies accumulate during the first day; they are far more numerous at 24 hours than at 2 hours. They are frequently seen connected with smooth endoplasmic reticulum (Figs. 10 and 23). Both the endoplasmic reticulum and membranous bodies show acid phosphatase activity (Figs. 12 and 13). These observations indicate that the membranous bodies arise from smooth endoplasmic reticulum.

During the first 3 days the mitochondria swell, round up, and lose their typical crista structure;

FIGURE 24 Portion of a nerve, 7 days after crush. The picture includes part of the nerve immediately distal to the crush and some of the foreign body reaction tissue (*RT*) which forms over the thread. Histiocytes (arrows) are numerous in the reaction tissue and are rare within the nerve (starred arrow). Histiocytes, because of their smaller size and dense accumulations of reaction product, are readily distinguishable from the transformed Schwann cells in the nerve fiber (*N*). (25 min.) $\times 400$.

FIGURE 25 Portion of same preparation as in Fig. 24. It demonstrates that the Schwann cells, when transformed, retain the linear arrangement they display in normal nerve, despite their shortening. Arrows indicate some of the vacuoles inside of which myelin fragments (not visible in the photograph) are undergoing degradation. Note reaction product at the periphery of some of these vacuoles and in numerous granules. $\times 900$.

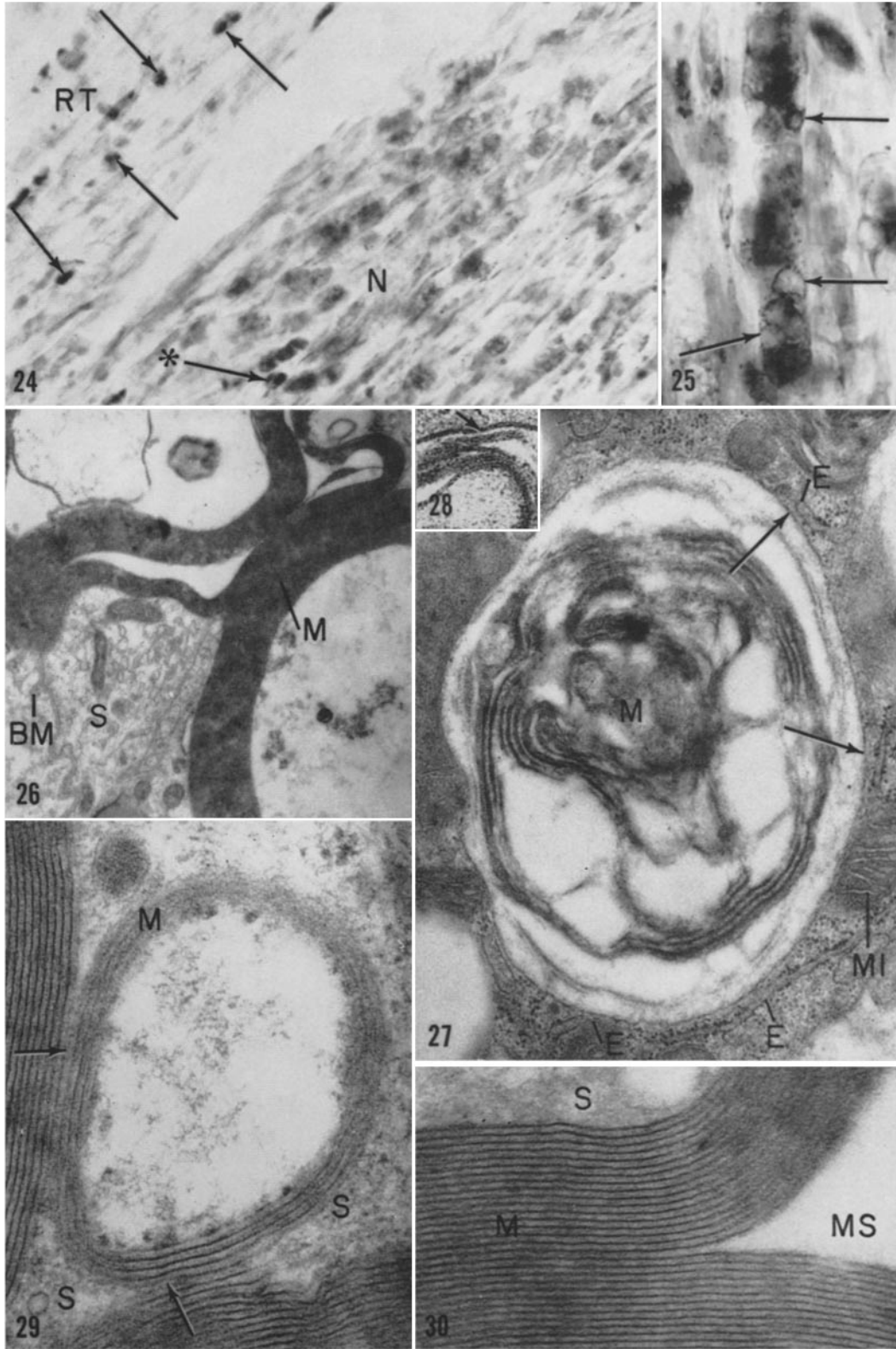
FIGURE 26 Portion of a transformed Schwann cell, 3 days after crushing. Schwann cell cytoplasm (*S*) has intruded within the myelin (*M*), thus separating a group of lamellae from the main body of myelin. Basement membrane (*BM*) is seen at the surface of the Schwann cell (*S*). $\times 13,000$.

FIGURE 27 Portion of a transformed Schwann cell, 3 days after crushing. It shows a vacuole containing degenerating myelin (*M*) and delimited by a single membrane that shows well at arrows. Note that the endoplasmic reticulum comes close to the vacuole periphery at *E*. A mitochondrion is seen at *MI*. $\times 40,000$.

FIGURE 28 Border of a similar vacuole in tissue fixed by glutaraldehyde perfusion and postfixed for 90 minutes in sodium permanganate. The "unit membrane" character of both the delimiting membrane (arrow) and myelin lamellae is evident. Lead stained. $\times 58,5000$.

FIGURE 29 Portion of a transformed Schwann cell, 3 days after crushing. A small fragment of myelin (*M*) has apparently separated from a larger fragment. Where the smaller fragment remains attached, intercalation of Schwann cell cytoplasm (*S*) is accompanied by splits in the major dense line (arrows). $\times 83,000$.

FIGURE 30 Portion of myelin fragment, 3 days after crushing. A space (*MS*) within the myelin fragment has separated the myelin (*M*) at the intermediate dense line. A small portion of the Schwann cell is seen at *S*. $\times 87,000$.



E. HOLTZMAN AND A. B. NOVIKOFF *Lysosomes in Rat Sciatic Nerve* 659

small bodies appear to separate from them (Figs. 14 and 23) (*cf.* references 2, 22, 23). Unlike the membranous bodies, the degenerating mitochondria show a capacity to bind lead. This is sometimes restricted to the dense intramitochondrial granules (Figs. 17 and 18) (*cf.* reference 24), but the lead is often present throughout the mitochondrion (Figs. 19 and 20).³ This lead-binding capacity is evident in material incubated in the Gomori medium with or without substrate. In contrast, the lead phosphate deposits in the endoplasmic reticulum and membranous bodies result from enzyme activity; they are present only when substrate (β -glycerophosphate) is in the incubation medium.

The focal accumulations of mitochondria, membranous bodies, and fragments of mitochondria sometimes appear to be paranodal, as described by Webster (2), but they are frequently seen throughout a considerable length of an inter-

³ Intramitochondrial granules which bind lead are encountered on some occasions in control (unoperated) unmyelinated fibers.

node. Axoplasm denuded of myelin is sometimes seen at the nodes of Ranvier. It is apparently left behind as the myelin retracts from the nodes to form the ovoids (Fig. 21) (*cf.* references 1, 25).

The cores seen in the light microscope correspond, in the electron microscope, to diffuse reaction product associated with virtually completely segregated neurofilaments (Figs. 22 and 23). They are seen most frequently toward the end of the first day. In most myelinated axons aggregation of the neurofilaments is less extreme (*cf.* references 25-27); thus distinct cores are not evident in the incubated sections. Shortly after their aggregation the neurofilaments are no longer identifiable (28-30).⁴

Electron microscopists (29, 31-37) have established, beyond reasonable doubt, that it is

⁴ It should be noted that neither axoplasmic granules nor "cores" are visualized when sections are incubated by the pararosaniline procedure for light microscope demonstration of acid phosphatase activity (38); instead, a diffuse reaction product forms in which organelles are not discernible.

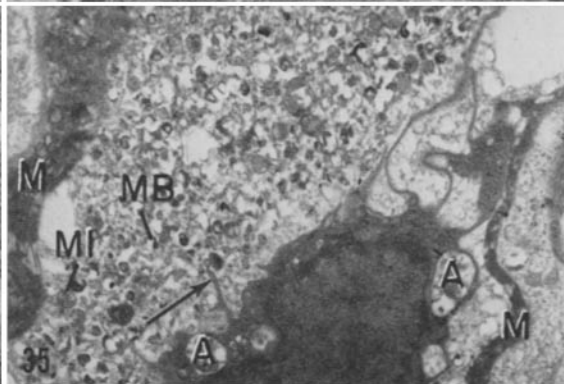
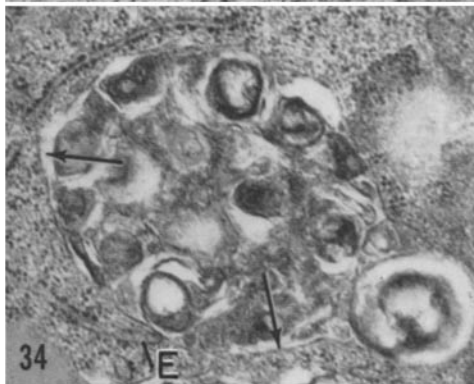
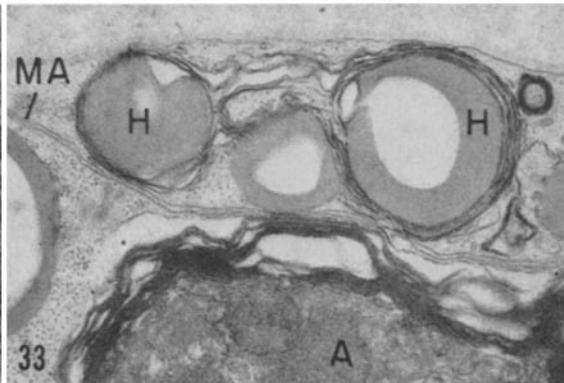
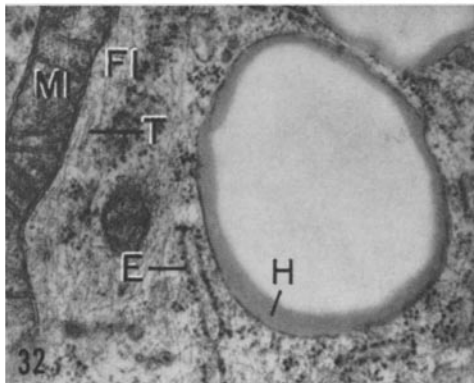
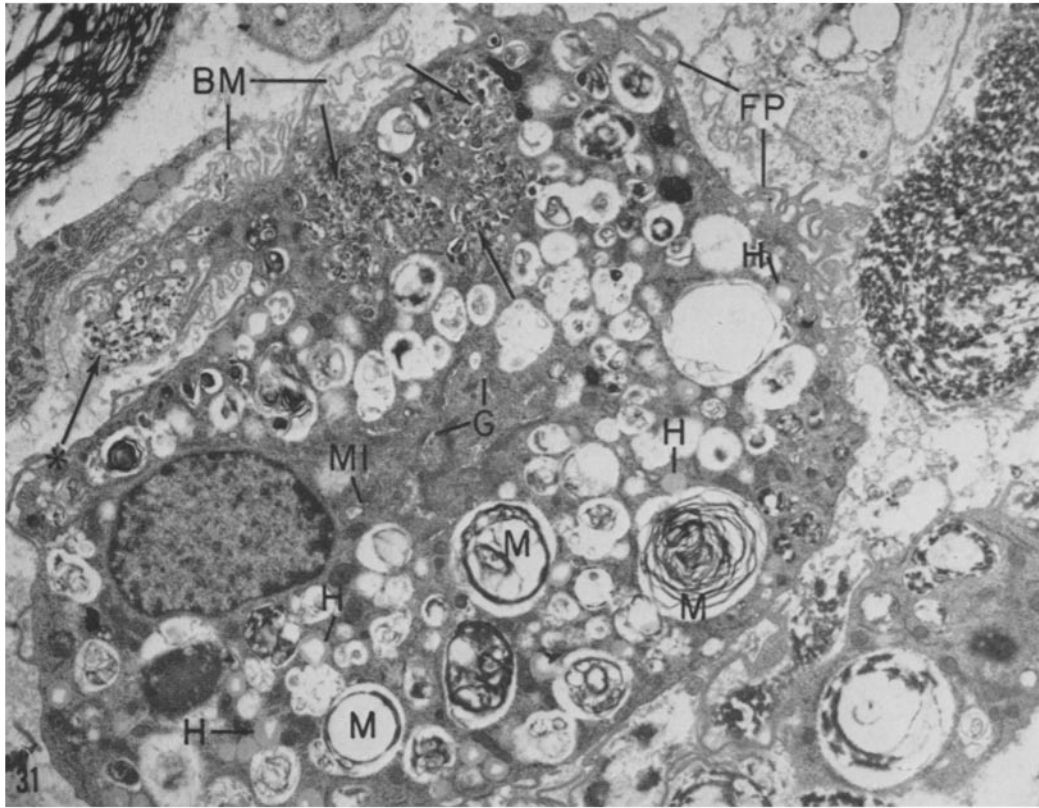
FIGURE 31 Portion of myelinated fiber, 3 days after crushing. Note ruffled basement membrane (*BM*) and numerous filopodia (*FP*) at the surface of the transformed Schwann cell occupying most of the field. The cell shows numerous myelin digestion vacuoles (*M*) and vacuoles with axoplasm (arrows). Some axoplasm is apparently being phagocytosed at the starred arrow. Barely evident at this magnification is the extensive Golgi apparatus (*G*) and mitochondria (*MI*). Note inclusions of homogeneous, moderately electron-opaque material (*H*), often lying near the myelin digestion vacuoles and sometimes connected to them (*cf.* Figs. 32 and 33). $\times 5000$.

FIGURE 32 Portion of a transformed Schwann cell in myelinated fiber, 3 days after crushing. Inclusion of homogeneous material (*H*) is seen more clearly than in Fig. 31. Note cisterna of rough endoplasmic reticulum (*E*), numerous fibrils (*FI*) (*cf.* reference 35), a microtubule (*T*), and a mitochondrion (*MI*). $\times 30,000$.

FIGURE 33 Portion of a transformed Schwann cell in myelinated fiber, 3 days after crushing. The homogeneous material (*H*) is surrounded by myelin lamellae. Note the persistent mesaxon (*MA*) and organelles in axoplasm (*A*) surrounded by a myelin fragment. Lead stained. $\times 26,000$.

FIGURE 34 Portion of same Schwann cell as in Fig. 31. Axoplasm is seen within a vacuole; note membrane at periphery of the vacuole (arrows). Endoplasmic reticulum is seen adjacent to the vacuole at *E*. $\times 33,000$.

FIGURE 35 Portion of a myelinated fiber, 3 days after crush. A cell has intruded within the degenerating myelin sheath (*M*). It is probably a transformed Schwann cell, although the possibility cannot be excluded that it is a histiocyte. Its filopodia appear to be engulfing axoplasmic material at arrow. Axoplasmic material is within vacuoles (*A*) that are about to separate or have already separated from the cell surface. Degenerating mitochondria (*MI*) and membranous bodies (*MB*) are seen in the denuded axoplasm. $\times 7500$.



within Schwann cells that the myelin is degraded during Wallerian degeneration and not within phagocytic vacuoles of invading histiocytes. This is also apparent from light microscope observation of acid phosphatase preparations. The Schwann cells shorten as they transform, but they retain their characteristic linear arrangement (Fig. 25). They acquire increasing numbers of lysosomes in the form of spheres with acid phosphatase product at their periphery (Fig. 25). However, they never appear as black in acid phosphatase preparations as do the histiocytes. Our surgical procedure favors the appearance of these histiocytes since a foreign body reaction occurs in response to the thread left at the crush. Most histiocytes remain in the foreign body reaction zone, but a few wander into the nerve. Because they are smaller and darker in acid phosphatase

preparations, they are readily detectable among the transformed Schwann cells (Fig. 24).

Myelin fragmentation begins at the nodes of Ranvier and the Schmidt-Lantermann clefts to produce the large segments or ovoids (1, 37). By intrusion of Schwann cell cytoplasm (Fig. 26) the ovoids are pinched into smaller masses with fewer lamellae. This separates the myelin lamellae at the major dense line (Fig. 29), corresponding to the cytoplasmic side of the plasma membrane of the Schwann cell prior to myelination (20).⁵ Eventually the myelin fragments are included in

⁵ The intermediate dense line, the original outer surface of the Schwann cell plasma membrane, often separates in our material (Fig. 30), as it does in osmotically swollen myelin (20); this produces spaces within the myelin (Fig. 30) (*cf.* references 39-41).

FIGURE 36 Portion of a transformed Schwann cell in myelinated fiber, 3 days after crushing. Several myelin lamellae are visible at the surface of the myelin digestion vacuoles (arrows). Five dense bodies are seen close to the vacuoles. Of these, two show electron-opaque grains similar to those seen in lysosomes of neurons, hepatocytes, and thyroid epithelium (44), and one contains a membranous array. Endoplasmic reticulum is adjacent to the digestion vacuoles in regions (*E*). $\times 38,000$.

FIGURE 37 Portion of a transformed Schwann cell in myelinated fiber, 3 days after crushing. Reaction product (arrow) is seen in association with the myelin (*M*), at the periphery of the digestion vacuoles, and in what appears to be the endoplasmic reticulum (starred arrows). More unequivocal conclusions regarding the endoplasmic reticulum require further study since: (*a*) after incubation, with our procedures, ribosomes do not show so well as in unincubated tissue; and (*b*) in some vacuoles more than one myelin lamella is found at the periphery (Fig. 36). (30 min.) $\times 35,000$.

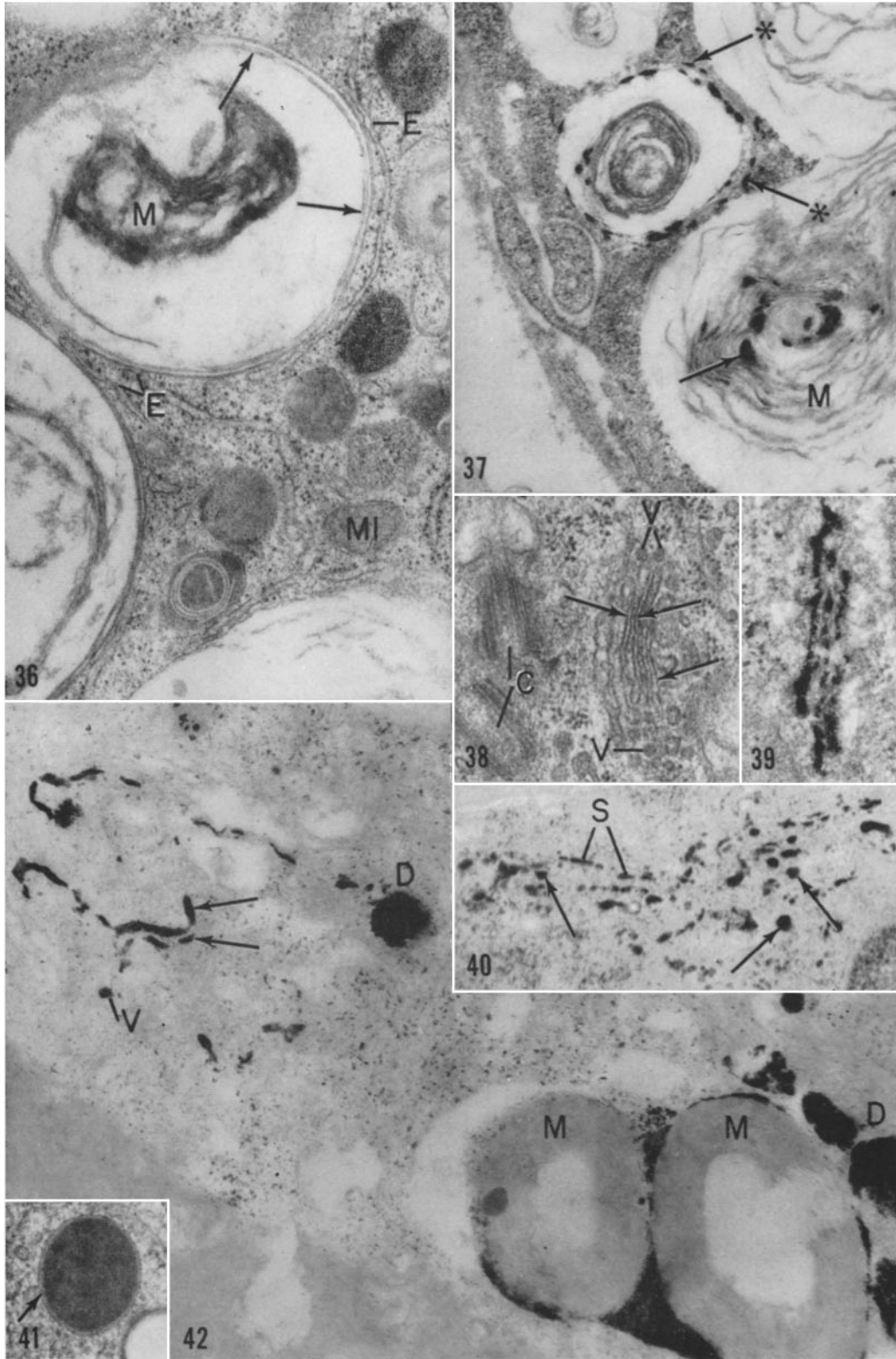
FIGURE 38 Portion of a transformed Schwann cell in myelinated fiber, 3 days after crushing. Note Golgi saccules (arrows), Golgi vesicles (*V*), and centrioles (*C*) (*cf.* reference 33). $\times 42,000$.

FIGURE 39 Portion of a Schwann cell in myelinated fiber, 2 hours after crushing. Three Golgi saccules show reaction product. (35 min.) $\times 43,000$.

FIGURE 40 Portion of a transformed Schwann cell in myelinated fiber, 7 days after crushing. Reaction product is present in Golgi saccules (*S*) and Golgi vesicles (arrows). (25 min.) $\times 26,000$.

FIGURE 41 A portion of a Schwann cell in a myelinated fiber of an unoperated nerve. Note the delimiting membrane (arrow) of the dense body. $\times 47,000$.

FIGURE 42 Portion of a transformed Schwann cell in myelinated fiber, 2 hours after crushing. Reaction product is associated with myelin fragments (*M*), dense bodies (*D*), Golgi saccules (arrows), and a Golgi vesicle (*V*). One dense body is close to the Golgi apparatus and several are close to the myelin digestive vacuole. Some non-specific deposition of lead is scattered throughout the section. Lead stained. (30 min.) $\times 38,000$.



digestion vacuoles within the Schwann cells (Figs. 27 and 31). These are often bounded by a single unit membrane (Figs. 27 and 28). In the course of myelin fragmentation Schwann cell cytoplasm is intercalated directly between myelin lamellae with no additional intervening membrane (Fig. 29). Thus the digestion vacuole membranes apparently derive from the myelin itself.⁶ Sometimes two or more myelin lamellae remain at the periphery (Fig. 36). We have also observed persistent mesaxons at the periphery of myelin fragments (Fig. 33) (*cf.* reference 31) and occasionally ordered periodic structures of various kinds including those reported by Thomas and Sheldon (42). As previous authors have reported (1, 42), axoplasmic material is often seen within the myelin fragments (Fig. 33).

By the third day the Schwann cells contain large numbers of myelin digestion vacuoles (Figs. 31 and 36). In addition, they show bodies made of a homogeneous material of moderate electron opacity, some of which is apparently removed during the preparation procedures for electron microscopy (Figs. 31 to 33). These homogeneous bodies often lie close to the digestion vacuoles (Fig. 31). Occasionally, vacuoles show both homogeneous material and myelin lamellae (Fig.

⁶ Other possibilities of delimiting membrane formation cannot be excluded. For example, on one occasion an image was seen that suggests participation of the endoplasmic reticulum in the formation of the membrane.

33), suggesting that the homogeneous material is a product of myelin digestion (*cf.* reference 43).

It is evident that the myelin is not phagocytosed in the usual manner. It is a part of the Schwann cell to start with, and throughout its fragmentation it remains within the cell. Our evidence clearly indicates that expulsion of myelin fragments and subsequent phagocytosis are not major phenomena, if they occur at all.

Fig. 37 shows that the digestion vacuoles in which myelin is degraded possess demonstrable acid phosphatase; they may thus tentatively be identified as lysosomes (7). Since the material undergoing degradation within them is a cytoplasmic entity, structured cell membrane or myelin, the digestion vacuoles may be considered to be cytolysosomes or autophagic vacuoles (6, 7, 44, 45). It is these vacuoles that are seen as spherical lysosomes by light microscopy (Fig. 25).

Endoplasmic reticulum frequently lies very close to the autophagic vacuoles (Figs. 27, 32, 34, and 36); it is not clear whether the regions near the vacuoles show acid phosphatase activity (see legend, Fig. 37). Not infrequently dense bodies are seen near the vacuoles (Figs. 36 and 42). They are membrane-delimited (Fig. 41) and possess demonstrable acid phosphatase activity (Fig. 42), and we therefore also consider them tentatively as lysosomes (7).

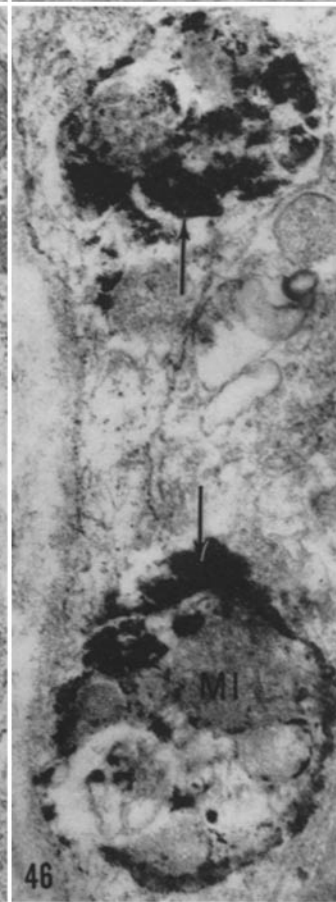
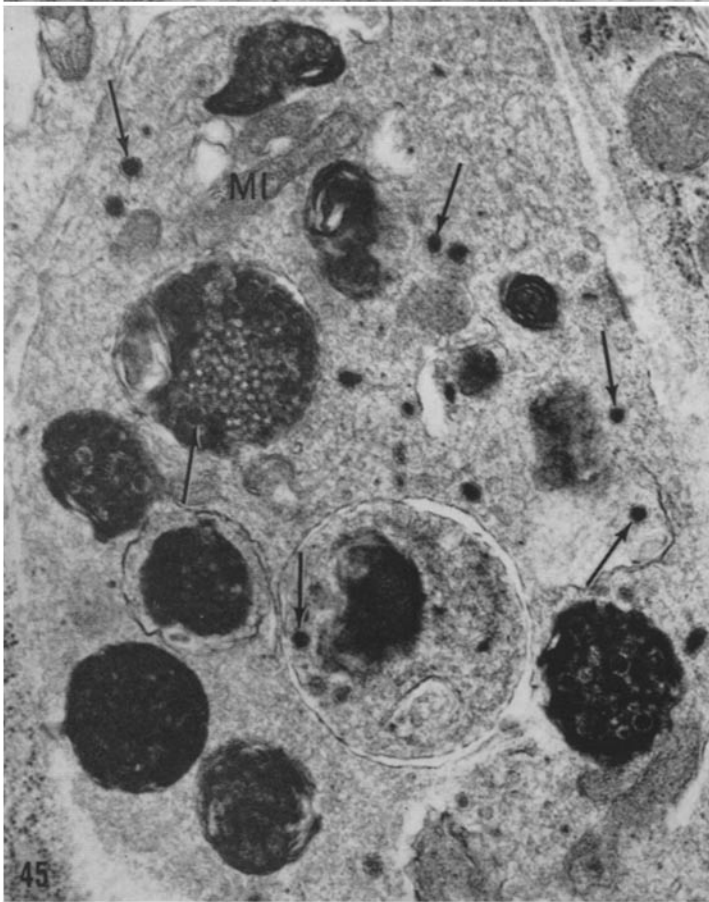
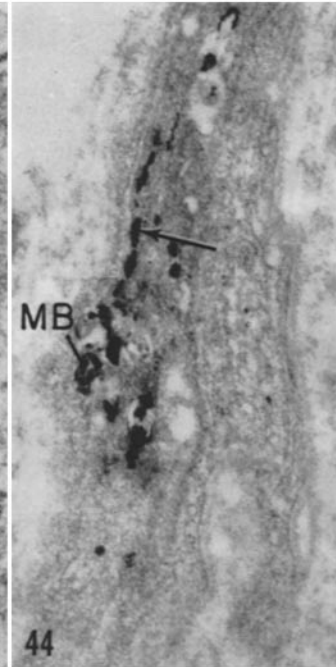
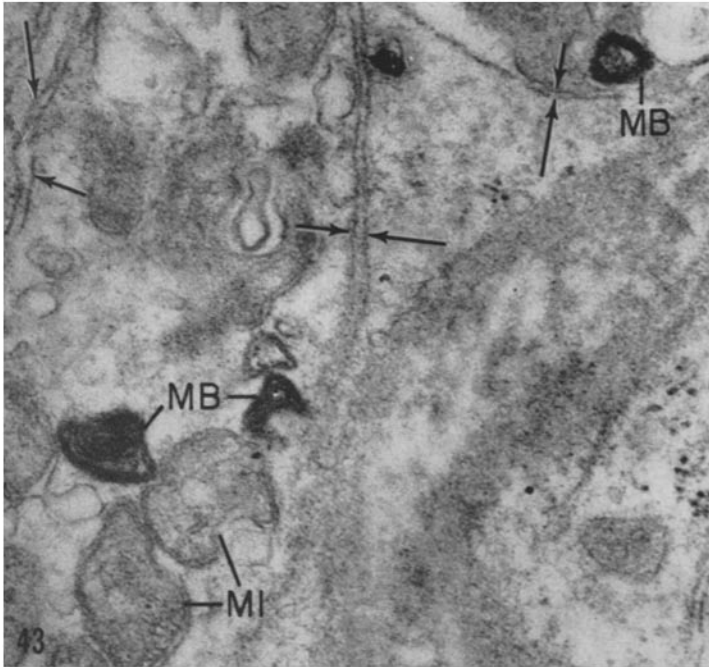
The Golgi apparatus of the Schwann cells is extensive and possesses many vesicles, presumably separating from the saccules (Fig. 38). At least some saccules and vesicles show acid phosphatase

FIGURE 43 Portion of an unmyelinated fiber, 1 day after crushing. Membranous bodies (*MB*), similar to those in myelinated fibers, are present in the axoplasm. Note mitochondria (*MI*) and plasma membranes of axoplasm (short arrows) and Schwann cells (long arrows). $\times 57,000$.

FIGURE 44 Portion of an unmyelinated fiber, 2 hours after crushing. Reaction product is present in the endoplasmic reticulum (arrow) and a membranous body (*MB*). (30 min.) $\times 23,500$.

FIGURE 45 Portion of a fiber in proximal segment of a nerve, 3 days after crushing. The axoplasm contains many dense inclusions. These include: (a) small membrane-delimited granules (*cf.* references 66, 67) (arrows); and (b) large autophagic vacuoles. The delimiting membranes show clearly in the three central vacuoles. Present within the vacuoles are small inclusion bodies (arrows) and electron-opaque material, some of which derives from degenerating mitochondria (*cf.* Fig. 46). A mitochondrion is seen at *MI*. $\times 37,500$

FIGURE 46 Portion of a fiber in proximal segment of a nerve, 3 days after crushing. Reaction product (arrows) is seen inside two autophagic vacuoles. Within the lower vacuole a recognizable mitochondrion is seen (*MI*). (30 min.) $\times 47,000$.



activity (Figs. 39, 40, and 42). This is of special interest because the Golgi vesicles have been proposed (7, 44, 46) as primary lysosomes (6).

The transformed Schwann cells often show numerous fine pseudopods or filopodia at their surface (Fig. 31). These occasionally appear to be engulfing masses of degenerating axoplasm into typical phagocytic vacuoles (Figs. 31, 34, and 35). This is axoplasm which has been exposed in the course of ovoid formation and myelin fragmentation. Sometimes, as in Fig. 31, phagocytic vacuoles containing axoplasm are seen in the same Schwann cells with numerous autophagic vacuoles containing myelin.

Unmyelinated Fibers

In general, the limited observations we have made on unmyelinated fibers suggest that they degenerate in the same way as myelinated fibers. Unoperated unmyelinated axons show acid phosphatase in relatively infrequent dense bodies and, rarely, in smooth endoplasmic reticulum. After crushing, the fibers show accumulations of acid phosphatase reaction product in the endoplasmic reticulum (Fig. 44) and in membranous bodies like those of myelinated fibers (Fig. 43; *cf.* reference 2). The formation of cores like those described in myelinated fibers has not been observed, although diffuse activity, not localized to any structure, is seen in some degenerating axons. The fragmentation of the unmyelinated fibers has been described by previous investigators (35, 48).

Proximal Segment

Extensive degeneration occurs in a short segment of the nerve immediately proximal to the crush. Our limited observations indicate that the accumulation of demonstrable acid phosphatase in the endoplasmic reticulum of the axoplasm and in the digestion vacuoles containing myelin occurs here as in the distal segment.

We were able to confirm the observations of Wettstein and Sotelo (26) that vacuoles containing degenerating cytoplasmic organelles appear early after crush in the proximal axoplasm. We observed them 2 to 3 days after crush. They are clearly membrane-delimited (Fig. 45) and they possess demonstrable acid phosphatase (Fig. 46). Thus, they may be considered lysosomes of the autophagic vacuole type (6, 7, 44, 45). We have not studied the origin of their delimiting membranes,

but the images seen are compatible with their origin from the endoplasmic reticulum.

DISCUSSION

Studies of pathological conditions such as those following nerve crush contribute much to the literature on lysosomes. No situation of which we are aware presents as vivid an array of lysosomes: primary lysosomes (Golgi vesicles in Schwann cells); dense bodies (in Schwann cells); membranous bodies (in axoplasm); autophagic vacuoles (in Schwann cells of distal nerve and in axoplasm of proximal nerve); phagocytic vacuoles (in altered Schwann cells and histiocytes of the foreign body reaction tissue) and others such as multivesicular bodies (in axoplasm) and small dense bodies (in Schwann cells near the nodes of Ranvier). Yet another mode of origin of delimiting membranes of autophagic vacuoles (*cf.* reference 49) is indicated, namely, from myelin lamellae. Nerve degeneration also adds a dramatic instance of increased acid phosphatase activity in the endoplasmic reticulum following injury. Other examples from our laboratory are the findings in hepatocytes of starved rats (44) and in KB cells following deprivation of arginine, an essential amino acid, or ultraviolet irradiation (50).

Numerous ribosomes are present and the endoplasmic reticulum is extensive in the transforming Schwann cells. It has been presumed (44, 49) that acid hydrolases are synthesized at the ribosomes and transported via the endoplasmic reticulum. Acid phosphatase reaction product in the endoplasmic reticulum has been seen in uninjured tissues: in some spinal cord neurons (51); in the ciliate *Cambanella* (47, 52); and in small neurons of dorsal root spinal ganglia (53). In the transformed Schwann cells, reaction product has not been observed in the endoplasmic reticulum generally, but the question is unanswered regarding that region of the endoplasmic reticulum adjacent to the autophagic vacuole, for reasons indicated in Fig. 37. In hepatocytes of starved rats, no activity is demonstrable in the endoplasmic reticulum generally but the regions near forming dense bodies do show it (reference 44, Fig. 18).

It is also not known whether the autophagic vacuoles of transformed Schwann cells obtain acid phosphatase from Golgi vesicles, some of which show acid phosphatase activity, or from acid phosphatase-rich dense bodies. The Golgi apparatus is extensive in altered Schwann cells (Figs. 38 to

40) but Golgi vesicles have not been observed to merge with the autophagic vacuoles. Dense bodies have been observed near the vacuoles (Figs. 36 and 42), but often vacuoles show no dense bodies nearby (serial sections were not studied).

How does the enzyme activity increase in the endoplasmic reticulum of distal axoplasm, separated from the ribosomes and other structures associated with protein synthesis in the perikaryon? It seems unlikely that the Schwann cells contribute enzyme to the endoplasmic reticulum of the axoplasm, particularly during the first hours after injury when the myelin sheath is largely unchanged. Possibly acid phosphatase is present in the normal nerve, but in inactive form, with activation occurring following injury. Activation of proteolytic enzymes (measured at pH 7.6), by *in vivo* "liberation" of enzyme, has been postulated by Adams and Tuqan (18) to account for the increase in activity during Wallerian degeneration. Yet another possibility is that the acid phosphatase is present in the unoperated nerve at a concentration too low to be demonstrable by current techniques, and that with the formation of membranous bodies the enzyme is somehow concentrated.

Attention has been called to lead binding by some degenerating mitochondria. This emphasizes the desirability of studying enzyme controls in which tissues are incubated in substrate-free media and in media containing inhibitors (sodium fluoride, in this instance). Other aspects of our findings direct attention to the factors influencing the precipitation of lead phosphate, about which too little information is currently available (*cf.* reference 54). Sometimes, the Schwann cells show no reaction product in the more distal part of the distal fiber. Yet it is reasonable to suppose that acid hydrolases are involved in myelin degradation in this region as in the more proximal part. If so, is the inability to reveal the presence of acid phosphatase due to inadequate fixation, with the region showing the enzyme activity only when adequately fixed? Or are unknown factors at play, factors that account also for the observation that acid phosphatase reaction product is often not present in other cell types at the time when digestion within vacuoles can reasonably be expected to be occurring (47, 52, 55, 56)? Indeed, even when reaction product is seen on degenerating myelin in the Schwann cells (*cf.* Fig. 37), it seems less in amount than might be expected.

The interpretation of the distribution of reaction product in cores (Figs. 5 and 22) needs to be qualified, since a diffuse distribution often reflects procedural inadequacies (54), and factors such as changed permeability of lysosomal membranes, following injury, might affect the precipitation of lead phosphate. The provisional interpretation is that the diffuse reaction product reflects release of acid phosphatase from the membranous bodies, with the free enzyme presumably playing a part in the degradation of axoplasmic constituents.

Methodological uncertainties may also complicate interpretation of the reaction product's absence in the axoplasm more distal to the crush. Nevertheless, electron microscope examination of this area in four nerves failed to reveal accumulations of membranous bodies at a time when the more proximal regions of the distal nerve show these acid phosphatase-rich bodies. Thus it seems probable that the absence of reaction product in the more distal zones reflects *in vivo* conditions. Conceivably, enzyme flows from distant portions of the axon proximally, toward regions nearer the crush, where it fills the endoplasmic reticulum and goes into newly formed membranous bodies. This flow (*cf.* reference 70) might also account for the marked acid phosphatase activity in fibers immediately adjacent to the crush (Fig. 6).

The listing of methodological uncertainties does not, in our opinion, becloud the positive identification of the various types of lysosomes in axoplasm and Schwann cell. Such identification raises questions of functional significance. For example, the autophagic vacuoles found in the proximal axoplasm shortly after severing the nerve are like those frequently seen when a tissue undergoes extensive reorganization (57-59). It is reasonable to expect that some of the smaller molecules, resulting from the digestion of macromolecules catalyzed by lysosomal hydrolases, will be utilized in the reorientation of metabolism which results later in regeneration (1, 4, 26, 60-62), *i.e.*, the outgrowth of new axoplasm. Similarly, it may become possible to ascertain if material resulting from the degradation of myelin and axoplasm inside the transformed Schwann cells is reutilized in the manifold activities of these cells prior to and during the downgrowth of new axoplasmic extensions.

This presentation illustrates again the results of examining an old problem with a fresh look. De Duve's concept of the lysosome (6) brings

added dimension to morphological observations of normal and pathological cells (7, 69). This is particularly true when morphology is supplemented by the cytochemical demonstration of one or more of the lysosomal enzymes. We trust that the uncertainties we have considered will not serve to make the statement of Cajal (1) apply to our interpretations. Commenting upon the important contributions of Waller earlier, he wrote, "Paradoxical as it may appear, it is certain that in the problem with which we are dealing, contrary to the usual course of science, error is modern while truth is ancient."

Dr. Holtzman is a recipient of a postdoctoral fellow-

ship from the National Institute of Neurological Diseases and Blindness.

This study was supported by a grant to Dr. Novikoff from the United States Public Health Service (CA-06576) and by a Research Career Award (5-K6-CA-14, 923) from the National Cancer Institute, United States Public Health Service.

The authors are indebted to Dr. H. Villaverde who performed the surgery, Miss R. Forschirm for preparation of the tissue sections, Mr. J. Godrich for preparing the photographs, and to Dr. S. Goldfischer for critical reading of the manuscript.

Portions of this material have been presented previously (21, 63, 64).

Received for publication, July 9, 1965.

REFERENCES

1. RAMON Y CAJAL, S., Degeneration and Regeneration of the Nervous System, (R. M. May, translator and editor), London, Oxford University Press, 2 volumes, 1928.
2. WEBSTER, H. DE F., *J. Cell Biol.*, 1962, **12**, 361.
3. LEE, J. C-Y., *J. Comp. Neurol.*, 1963, **120**, 65.
4. LAMPERT, P., and CRESSMAN, M., *Lab. Inv.*, 1964, **13**, 825.
5. TANI, E., *J. Neuropath. and Exp. Neurol.*, 1964, **23**, 162.
6. DE DUVE, C., Ciba Foundation Symposium on Lysosomes, (A. V. S. de Reuck and M. P. L. Cameron, editors), Boston, Little, Brown and Company, 1963, 1.
7. NOVIKOFF, A. B., Ciba Foundation Symposium on Lysosomes, (A. V. S. de Reuck and M. P. L. Cameron, editors), Boston, Little, Brown and Company, 1963, 36.
8. SABATINI, D. D., BENSCH, K., and BARNETT, R. J., *J. Cell Biol.*, 1963, **17**, 19.
9. WEBSTER, H., DE F., and COLLINS, G. H., *J. Neuropath. and Exp. Neurol.*, 1964, **23**, 109.
10. GOMORI, G., Microscopic Histochemistry, Chicago, University of Chicago Press, 1952.
11. GOULD, R. P., and HOLT, S. J., in Proceedings of the Anatomical Society of Great Britain and Ireland, London, Taylor and Francis, Ltd., 1961, 45.
12. PALADE, G. E., *J. Exp. Med.*, 1952, **95**, 285.
13. LUFT, J. H., *J. Biophysic. and Biochem. Cytol.*, 1961, **9**, 409.
14. ROSENBLUTH, J., *J. Cell Biol.*, 1963, **16**, 143.
15. WATSON, M. L., *J. Biophysic. and Biochem. Cytol.*, 1958, **4**, 475.
16. REYNOLDS, E. S., *J. Cell Biol.*, 1963, **17**, 208.
17. LEHMANN, H., *Z. Zellforsch. u. Mikr. Anat.*, 1960, **51**, 283.
18. ADAMS, C. W. M., and TUQAN, N. A., *J. Neurochem.*, 1961, **6**, 334.
19. ANDERSON, P. J., and SONG, S. K., *J. Neuropath. and Exp. Neurol.*, 1962, **21**, 263.
20. ROBERTSON, J. D., *Progr. in Biophysic. and Biophysic. Chem.*, 1960, **10**, 343.
21. NOVIKOFF, A. B., Abstracts of 62nd Annual Meeting of American Association of Pathology and Bacteriology, Philadelphia, March, 1965, *Am. J. Path.*, 1965, **46**, 4a.
22. LAMPERT, P., BLUMBERG, J. M., and PENTSCHEW, A., *J. Neuropath. and Exp. Neurol.*, 1964, **23**, 60.
23. SCHLAEPFER, W. W., and HAGER, H., *Am. J. Path.*, 1964, **45**, 209, 423.
24. PEACHEY, L. D., *J. Cell Biol.*, 1964, **20**, 95.
25. ANDRES, K. H., *Z. Zellforsch. u. Mikr. Anat.*, 1963, **61**, 1.
26. WETTSTEIN, R., and SOTELO, J. R., *Z. Zellforsch. u. Mikr. Anat.*, 1963, **59**, 708.
27. TERRY, R. D., and PENA, C., *J. Neuropath.*, 1965, **24**, 200.
28. VIAL, J. D., *J. Biophysic. and Biochem. Cytol.*, 1958, **4**, 551.
29. OHMI, S., *Z. Zellforsch. u. Mikr. Anat.*, 1961, **54**, 39.
30. WECHSLER, W., and HAGER, H., *Beiter. Path. Anat. u. allg. Path.*, 1962, **126**, 352.
31. GLIMSTEDT, G., and WOHLFART, G., *Acta Morphol. Neerl. Scand.*, 1960, **3**, 135.
32. PALMER, E., REES, R. J. W., and WEDDELL, G., in Proceedings of the Anatomical Society of Great Britain and Ireland, London, Taylor and Francis, Ltd., 1961, 49.
33. BARTON, A. A., *Brain*, 1962, **85**, 799.
34. FISHER, E. R., and TURANO, A., *Arch. Path.*, 1963, **75**, 517.

35. NATHANIEL, E. J. H., and PEASE, D. C., *J. Ultrastruct. Research*, 1963, **9**, 511.
36. THOMAS, P. K., *J. Cell Biol.*, 1964, **23**, 375.
37. WEBSTER, H DE F., *Ann. New York Acad. Sc.*, 1965, **122**, 29.
38. BARKA, T., and ANDERSON, P. J., *J. Histochem. and Cytochem.*, 1962, **10**, 741.
39. FINEAN, J. B., and WOOLF, A. L., *J. Neuropath. and Exp. Neurol.*, 1962, **21**, 105.
40. ALEU, F. P., KATZMAN, R., and TERRY, R. D., *J. Neuropath. and Exp. Neurol.*, 1963, **22**, 403.
41. GONATAS, N. K., LEVINE, S., and SHOULSON, R., *Ann. New York Acad. Sc.*, 1965, **122**, 6.
42. THOMAS, P. K., and SHELDON, H., *J. Cell Biol.*, 1964, **22**, 715.
43. TERRY, R. D., and HARKIN, J. C., *The Biology of Myelin*, (S. Korey, editor), New York, Paul B. Hoeber, Inc., 1959, 303.
44. NOVIKOFF, A. B., ESSNER, E., and QUINTANA, N., *Fed. Proc.*, 1964, **23**, 1010.
45. SWIFT, H., and HRUBAN, Z., *Fed. Proc.*, 1964, **23**, 1026.
46. BRANDES, D., *J. Ultrastruct. Research*, 1965, **12**, 63.
47. CARASSO, N., GOLDFISCHER, S., and FAVARD, P., *J. Micr.* 1964, **3**, 297.
48. TAXI, J., *Compt. rend. Acad. Sc.*, 1959, **248**, 2796.
49. NOVIKOFF, A. B., and SHIN, W.-Y., *J. Micr.*, 1964, **3**, 187.
50. LANE, N. J., and NOVIKOFF, A. B., *J. Cell Biol.*, 1965, **27**, 603.
51. NOVIKOFF, A. B., ESSNER, E., and QUINTANA, N., *J. Micr.*, 1963, **2**, 3.
52. GOLDFISCHER, S., CARASSO, N., and FAVARD, P., *J. Micr.*, 1963, **2**, 621.
53. NOVIKOFF, A. B., QUINTANA, N., VILLAVERDE, H., and FORSCHIRM, R., *J. Cell Biol.*, 1964, **23**, 68A.
54. HOLT, S. J., *Exp. Cell Research, Suppl.*, 1959, **7**, 1.
55. WETZEL, B. K., HORN, R. G., and SFIGER, S. S., *J. Histochem. and Cytochem.*, 1963, **11**, 814.
56. MILLER, F., and PALADE, G. E., *J. Cell Biol.*, 1964, **23**, 519.
57. MOE, H., and BEHNKE, O., *J. Cell Biol.*, 1962, **13**, 168.
58. BEHNKE, O., *J. Cell Biol.*, 1963, **18**, 251.
59. BALIS, J. U., and CONEN, P. E., *Lab. Inv.*, 1964, **13**, 1215.
60. NATHANIEL, E. J. H., and PEASE, D. C., *J. Ultrastruct. Research*, 1963, **9**, 533.
61. McCAMEN, R. E., and ROBBINS, E., *J. Neurochem.*, 1959, **18**, 32.
62. NOBACK, C., and REILLY, J. A., *J. Comp. Neurol.*, 1952, **105**, 333.
63. HOLTZMAN, E., NOVIKOFF, A. B., and VILLAVERDE, H., Abstracts, 16th Annual Meeting of the Histochemical Society, Philadelphia, April, 1965, *J. Histochem. and Cytochem.*, 1965, **13**, 705.
64. NOVIKOFF, A. B., and HOLTZMAN, E., Abstracts, 41st Annual Meeting of the American Association of Neuropathology, Atlantic City, June, 1965, *J. Neuropath. and Exp. Neurol.*, 1966, **25**, 130.
65. SANDBORN, E., KOEN, P. F., McNABB, J. D., and MOORE, G., *J. Ultrastruct. Research*, 1964, **11**, 123.
66. PALAY, S. L., *Anat. Rec.*, 1960, **138**, 417.
67. ROSENBLUTH, J., *Z. Zellforsch. u. Mikr. Anat.*, 1963, **60**, 213.
68. DE REUCK, A. V. S., and CAMERON, M. P. L., editors, *Ciba Symposium on Lysosomes*, Boston, Little, Brown and Company, 1963.
69. NOVIKOFF, A. B., *Progr. in Brain Research*, in press.
70. LUBINSKA, L., *Progr. in Brain Research*, 1964, **13**, 1.